Geophysical Journal International

Geophys. J. Int. (2023) **235,** 2323–2338
Advance Access publication 2023 September 26
GJI Applied and Marine Geophysics

https://doi.org/10.1093/gji/ggad367

Heat extraction calculations for deep coaxial borehole heat exchangers: matrix analytical approach

Ctirad Matyska[1] and Eliška Zábranová[2]

[1] *Department of Geophysics, Faculty of Mathematics and Physics, Charles University,* 180 00 *Prague* 8, *Czech Republic. E-mail: Ctirad.Matyska@mff.cuni.cz*
[2] *Institute of Rock Structure and Mechanics, Czech Academy of Sciences,* 180 00 *Prague* 8, *Czech Republic*

Accepted 2023 September 18. Received 2023 July 5; in original form 2023 February 9

SUMMARY

Deep boreholes represent a source of clean energy. Therefore, effective calculations of potential extraction of heat from boreholes for realistic models of the Earth's crust with variable thermal conductivity and diffusivity are needed. We deal with heat extraction in a quasi-steady state from coaxial boreholes where downward and upward flows of pumped fluid (water) are separated by an inner pipe and connected only at the bottom. We first obtain theoretical estimates of heat extraction for a thermally isolated inner pipe and a model of the ground with constant thermal diffusivity and conductivity. Then, we develop a new analytical matrix method for a general layered ground model that enables us to include depth-dependent ground properties as well as heat exchange between the downward and upward flows of fluid in the borehole. Our straightforward and fast approach is thus suitable for various parametric studies or as a tool for benchmarks of numerical software. A key role in heat extraction from coaxial boreholes is played by the inner-pipe thermal resistance. We apply our method to the parametric study showing the dependence of pumped water temperature and total heat extraction from the borehole on realistic borehole geometries under different amounts of water pumping. The calculations are performed for a 3 km deep borehole as the representative of present deep boreholes used for extraction of geothermal energy and for a 10 km deep borehole. Drilling of such a superdeep borehole has just started in China and our results demonstrate potential limits of geothermal energy extraction from such great depths.

Key words: Numerical approximations and analysis; Heat flow; Hydrothermal systems.

1 INTRODUCTION

Numerical estimates dealing with the potential extraction of heat from boreholes have a long tradition going back to the 80s of the last century (Eskilson 1987). For example, Claesson and Eskilson (1988) studied heat extraction from boreholes if the temperature at the borehole wall is known (estimated); that is, only the heat flow conduction equation outside the borehole is (analytically) solved for prescribed boundary conditions. However, we need to couple heat conduction outside boreholes with heat convection due to the flowing fluid inside boreholes to be able to study more general situations.

In this study, we concentrate on coaxial heat exchangers, where cold fluids flow downward in an annular pipe, extracting heat from the surrounding rock through the borehole wall and grout, change direction at the bottom of the borehole and flow upward in a central pipe, which is mechanically isolated from the annular pipe. The straightforward approach to this problem is based on fully 2-D numerical modelling in axial geometry, where the finite-element method (FEM), the finite-difference method (FDM), or the finite-volume method (FVM) can be applied. For example, the FEM was used to estimate the maximal potential heat extraction from the 2302 m deep borehole at Weggis in Switzerland (Kohl *et al.* 2002), and, similarly, for a 5 km deep borehole heat exchanger, where groundwater velocity was also taken into account (Le Lous *et al.* 2015). Detailed methodological papers dealing with the FEM employing the FEFLOW–TRNSYS software were published by Diersch *et al.* (2011a, b). Popular FEM open software enabling to solve, inter alia, the problem of heat extraction from coaxial heat exchangers, is OpenGeoSys (Cai *et al.* 2022; Brown *et al.* 2023a, b). The FVM was, for example, employed by Iry and Rafee (2019) to study the thermal and hydrodynamic performance of the coaxial borehole heat exchanger in transient regimes for different borehole diameters. The advantage of fully numerical methods is that they can naturally deal with models of the ground that change with depth. However, such a full numerical approach is computationally demanding because the radial spatial resolution in a borehole and its vicinity must be very high compared to the depth extent of the model.

Therefore, it is numerically advantageous to deal with the case where the interaction of a coaxial borehole with the surrounding ground is studied under the assumption that the heat transfer in the circulating fluid is approximated by a 1-D energy balance equation. Recently, new papers have appeared that study this problem. To solve this simplified coupled problem numerically, the FDM was used in Fang *et al.* (2018), Song *et al.* (2018), Morchio and Fossa (2019) and Li *et al.* (2021), while the FVM was employed in He and Bu (2020) and Liu *et al.* (2020). On the other hand, Pan *et al.* (2020) solved the problem by using the analytical approach in the Laplace transform domain, similarly as Beier *et al.* (2014), followed by a numerical inverse Laplace transform algorithm to obtain the solution. An extensive review of experimental, numerical and analytical approaches to estimate the extraction of heat from the ground by employing coaxial heat exchangers can be found in Ma *et al.* (2020).

However, there are also attempts to develop (quasi-)analytical approaches in a time domain. Pan *et al.* (2019) analytically solved ordinary differential equations describing the thermal balance of the circulating fluid in the outer and inner pipes of a coaxial borehole under the strong simplifying assumption of constant temperature at the borehole wall. Luo *et al.* (2019, 2020, 2022) combined a steady-state analytical model for a flowing fluid with an analytical transient heat conduction model of the ground surrounding the borehole, which is based on a segmented finite line source model. Similar approach was used also in a complex study by Jiao *et al.* (2021). Ma *et al.* (2020) analytically expressed the heat conduction in the surrounding ground, where the heat flow or temperature at the borehole wall are unknown quantities that are determined together with the temperature of the outflowing fluid. They propose iteration schemes, where either the total energy balance or temperature smoothness criteria are used to stop the algorithm. Their approach is designed for a general layered model. Zhao *et al.* (2020) used similarly the analytical expression for heat conduction outside the borehole, but the energy balance for flowing fluid solved by a finite-difference scheme. Their approach is also iterative, since the outflow temperature is found by minimizing error in the total energy balance of the problem. The analytical approach for a layered model was published by Karabetoglu *et al.* (2021), also for the case, when the temperature at the borehole wall is estimated *a priori*.

The main motivation of this paper is to show that in a case of quasi-steady-state approximation, the problem of heat extraction from coaxial boreholes in layered ground models can be fully solved analytically, and the only part of the solution that requires more (but still fast) numerical calculations is the evaluation of series of the Bessel functions that describe heat conduction in the ground outside a borehole. Moreover, this part is solved independently and its results can be used repeatedly for several parametric studies. The software based on our formulae is thus fast and efficient. The problem is solved for general layered models, where all quantities characterizing the model (i.e. the physical parameters of the ground, the geothermal gradient and the thermal resistances of the pipe and borehole walls) are constant in each layer. Since the thickness of each layer is another free parameter, our approach enables us to deal with models that change with depth in a general way. In each of the layers, the heat conduction outside the borehole is expressed similarly as in Ma *et al.* (2020) and Zhao *et al.* (2020), and coupled with a quasi-steady-state analytical solution for temperature changes of both the downward and upward flows of the fluid inside the borehole. The analytical solutions within the layers are subsequently coupled by a matrix method that employs the continuity of the fluid temperature at the layer interfaces. By adding appropriate boundary conditions, we finally receive a complete analytical solution of the problem, where no additional iterations are needed. We present formulae for the cases, where input controlling parameter is the temperature of inflowing water or the total heat extraction or the temperature of outflowing water. We also explicitly show that the problem is even substantially simpler if the upward hot fluid can be considered as thermally isolated from the colder fluid flowing downward and the thermal resistance between the downward flowing water and the ground is negligible. Such an approximation is suitable for maximum estimates of potential heat extraction from a borehole.

2 METHOD

The problem consists of the two parts that are solved separately. In the first part, we will deal with heat conduction outside a borehole and in the second part, we will describe energy balance between heat conduction in the ground and water circulating in the borehole.

2.1 Temperature and heat flow outside the borehole

We consider the case where the heat conductivity k, density ρ and the heat capacity c_p of the crust depend only on the depth z. Radial distance from the centre of the borehole is denoted by r and its radius by r_a, respectively. Groundwater advection is neglected, and thus only heat conduction is considered outside the borehole $r > r_a$, that is,

$$\rho c_p \frac{\partial T}{\partial t} = \nabla \cdot (k \nabla T), \tag{1}$$

where $T(r, z, t)$ is the temperature and t is the time.

In the case of *constant material properties*, eq. (1) simplifies to

$$\frac{\partial T}{\partial t} = \kappa \nabla^2 T, \tag{2}$$

where $\kappa \equiv k/\rho c_p$ is the thermal diffusivity and

$$\nabla^2 \equiv \frac{1}{r}\frac{\partial}{\partial r}\left(r\frac{\partial}{\partial r}\right) + \frac{\partial^2}{\partial z^2},$$

is the Laplace operator expressed in the cylindrical coordinates r and z. Furthermore, in the case of the fluid circulating in the borehole, radial conduction dominates in its vicinity, that is, $|\partial T/\partial z| \ll |\partial T/\partial r|$, see also Ma *et al.* (2020) and Zhao *et al.* (2020). This assumption is well justified. For example, Cai *et al.* (2022) showed that the thermal influencing radius of the boreholes is only about 30 m for relatively long 15 yr of operation. The horizontal temperature gradients are thus of the order of several $^\circ$C m^{-1}, whereas typical vertical temperature gradients far from the borehole are about two orders of magnitude smaller. Moreover, the vertical temperature gradient at the borehole wall is even smaller due to the cooling of the wall by the downflowing water. Eq. (2) thus attains the form

$$\frac{\partial T}{\partial t} = \frac{\kappa}{r}\frac{\partial}{\partial r}\left(r\frac{\partial T}{\partial r}\right) . \tag{3}$$

We take into account the boundary conditions $T = T_a(z)$ if $r = a$ and $T = T_b(z)$ if $r = b$, where $b \gg a$ represents the boundary of the computational domain. Zhao *et al*. (2020) analysed in detail how the outside boundary radius b should be large to prevent false heat flow due to the (artificial) external boundary condition. Substantial reduction of the computational domain up to tens of metres in radial direction is advantageous since the numerical evaluation of the series of Bessel functions solving the eq. (3, see below) is then more efficient. The initial condition for $t = 0$ is $T = T_b$.

Solution of eq. (3) satisfying the considered boundary and initial conditions can be found by means of the formulae published in Carslaw and Jaeger (1959):

If we express the temperature T in the form

$$T = \frac{T_a \ln(b/r) + T_b \ln(r/a)}{\ln(b/a)} + u(r)\exp\left(-\kappa\alpha^2 t\right) , \tag{4}$$

the function $u(r)$ must satisfy the boundary conditions $u(a) = u(b) = 0$ and the equation

$$\frac{\mathrm{d}^2 u}{\mathrm{d}r^2} + \frac{1}{r}\frac{\mathrm{d}u}{\mathrm{d}r} + \alpha^2 u = 0 , \tag{5}$$

which is the Bessel equation of order zero. The corresponding solutions are the Bessel functions of the first and second kind that will be denoted by $J_0(\alpha r)$ and $Y_0(\alpha r)$. $u(r)$ can be expressed as the combination of the Bessel functions

$$u(r) = J_0(\alpha r)Y_0(\alpha b) - J_0(\alpha b)Y_0(\alpha r) \equiv U_0(\alpha r) , \tag{6}$$

the boundary condition $u(b) = 0$ is already fulfilled and the boundary condition $u(a) = 0$ is then satisfied for such α_n that are the roots of the equation

$$J_0(\alpha a)Y_0(\alpha b) - J_0(\alpha b)Y_0(\alpha a) = 0 . \tag{7}$$

After some algebra (Carslaw and Jaeger 1959, pp. 206–207), one finally gets

$$T = \frac{T_a \ln(b/r) + T_b \ln(r/a)}{\ln(b/a)} - \pi\sum_{n=1}^{\infty}\frac{\{T_b J_0(a\alpha_n) - T_a J_0(b\alpha_n)\}J_0(a\alpha_n)U_0(r\alpha_n)}{J_0^2(a\alpha_n) - J_0^2(b\alpha_n)}\exp\left(-\kappa\alpha_n^2 t\right)$$
$$+ T_b\pi\sum_{n=1}^{\infty}\frac{J_0(a\alpha_n)U_0(r\alpha_n)}{J_0(a\alpha_n) + J_0(b\alpha_n)}\exp\left(-\kappa\alpha_n^2 t\right) , \tag{8}$$

where the first term is the stationary solution $T_s(r)$ of eq. (3) satisfying non-homogeneous boundary conditions $T_s(a) = T_a$, and $T_s(b) = T_b$, the second term solves eq. (3) with zero boundary conditions and initial condition $T(r, 0) = -T_s(r)$. This second particular solution of the eq. (3) then enables to obtain the solution with zero initial condition simultaneously satisfying the boundary conditions—it is represented by the sum of these two terms. Finally, the third term is the solution of eq. (3) with zero boundary conditions and initial condition $T = T_b$ and thus the sum of these three terms satisfies eq. (3) together with the required boundary conditions.

Rewrite now $T = T_a + \Delta T$. ΔT is again the solution of eq. (3), but with the boundary conditions $\Delta T(a) = 0$ and $\Delta T(b) = T_b - T_a$, that is, using eq. (8) we can immediately write ΔT as

$$\Delta T = (T_b - T_a)\frac{\ln(r/a)}{\ln(b/a)} - \pi\sum_{n=1}^{\infty}\frac{(T_b - T_a)J_0^2(a\alpha_n)U_0(r\alpha_n)}{J_0^2(a\alpha_n) - J_0^2(b\alpha_n)}\exp\left(-\kappa\alpha_n^2 t\right) + (T_b - T_a)\pi\sum_{n=1}^{\infty}\frac{J_0(a\alpha_n)U_0(r\alpha_n)}{J_0(a\alpha_n) + J_0(b\alpha_n)}\exp\left(-\kappa\alpha_n^2 t\right) . \tag{9}$$

Close to the borehole, that is, for $r \ll b$ and the small time t compared to the diffusion time $(b - a)^2/\kappa$, the first two terms in relation (9) are negligible, and

$$T(r, z, t) \to T_a(z) + (T_b(z) - T_a(z))\pi\sum_{n=1}^{\infty}\frac{J_0(a\alpha_n)U_0(r\alpha_n)}{J_0(a\alpha_n) + J_0(b\alpha_n)}\exp\left(-\kappa(z)\alpha_n^2 t\right) . \tag{10}$$

The heat flow $q = k\,\partial T/\partial r$ (in W m^{-2}) at the external boundary of the borehole $r = a$ is, therefore,

$$q(a, z, t) = k(z)(T_b(z) - T_a(z))\pi\sum_{n=1}^{\infty}\frac{\alpha_n J_0(a\alpha_n)U_0'(a\alpha_n)}{J_0(a\alpha_n) + J_0(b\alpha_n)}\exp\left(-\kappa(z)\alpha_n^2 t\right) , \tag{11}$$

where U_0' is the derivative of the function U defined in eq. (6).

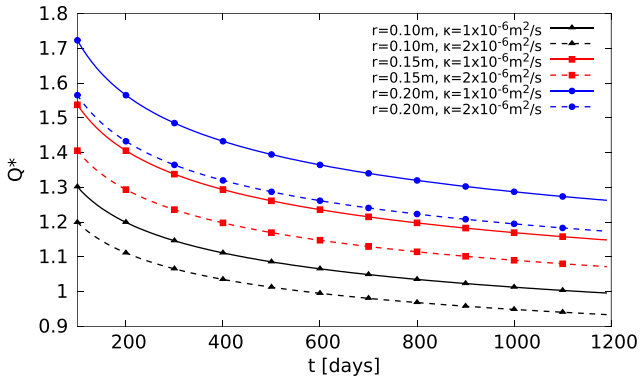

Figure 1. Dimensionless quantity $Q^*(t) \equiv Q'(t)/(k(T_b - T_a))$ for $\kappa = 1.0$, and 2.0×10^{-6} m^2 s^{-1} and the three values of the borehole radii 0.1, 0.15 and 0.2 m.

In the above equations, $T_a(z)$ is not dependent on time. However, we will deal with models, where the temperature T_a starts from $T_b(z)$ at the initial time $t = 0$, gradually decreases with time, and the quasi-steady-state approximation for evaluation of the total heat flow Q' passing through 1 m of the borehole length, formally consistent with eq. (11), can be applied, that is,

$$Q'(a, z, t) \doteq k(z)(T_b(z) - T_a(z, t))Q^*(a, z, t)\,, \tag{12}$$

where

$$Q^*(a, z, t) = 2\pi^2 a \sum_{n=1}^{\infty} \frac{\alpha_n J_0(a\alpha_n) U_0'(a\alpha_n)}{J_0(a\alpha_n) + J_0(b\alpha_n)} \exp\left(-\kappa(z)\alpha_n^2 t\right)\,. \tag{13}$$

Since the product $a\alpha_n$ is dimensionless, Q^* is also dimensionless. We see that Q' is expressed in W m^{-1}, if k is expressed in W mK^{-1} and $T_b - T_a$ in K, respectively. Fig. 1 shows the numerically calculated dimensionless quantity Q^* in days for several radii a of the borehole and two thermal diffusivities. One can clearly see that after several months $Q^* \gtrsim 1$, and the subsequent decrease with time is very slow. Emphasize that the relation (12) is crucial for our method, since it will enable us to solve the problem analytically in homogeneous layers, see the text in Section 2.2.

Rough estimates of maximal heat extraction from deep boreholes can easily be done without additional calculations: if we consider k to be about 3 W mK^{-1}, $Q'/(T_b - T_a) \equiv kQ^*$ is typically about 4 W mK^{-1} for $a = 0.15$ m, $\kappa = 10^{-6}$ m^2 s^{-1} and times around one year. Furthermore, if the background temperature gradient $\mathrm{d}T_b/\mathrm{d}z$ is approximately 0.03 K m^{-1} and $T_a(z)$ is considered close to the averaged ground surface temperature T_0 (which can be reached by sufficiently intensive pumping of a fluid of the same temperature T_0 into the borehole), we get a rough estimate of the total heat extraction Q_{tot} from the borehole in a quasi-steady-state case after several months (in W),

$$Q_{\mathrm{tot}} \sim 4 \times (0.015\, d) \times d\,, \tag{14}$$

where d is the total depth of the borehole (in m) and $0.015\, d$ is the average value of $T_b - T_a$ (in K), since for linearly increasing temperature with gradient β its average temperature between surface and the depth d is $\beta d/2$. Therefore, *the maximum theoretical heat extraction* from the borehole is approximately quadratically increasing with depth d. For example, for the borehole reaching 2 km depth we get the estimate $Q_{\mathrm{tot}} \sim 240$ kW and for a very deep borehole reaching a depth of about 7 km, $Q_{\mathrm{tot}} \sim 3$ MW according to eq. (14). It is clear that for a superdeep borehole reaching the depth of about 10 km, the estimate of the background temperature gradient should decrease, but still several MW seems to be the reasonable estimate of maximum heat extraction.

These rough estimates are in a good agreement with those published in literature. For example, Fang *et al.* (2018) obtained for the 2 km deep borehole with the same values of k and the geothermal gradient similar estimate (300 kW) for the maximal heat extraction in quasi-steady state. However, their model was based on full 3-D numerical modelling of coupled heat advection in circulating water with heat conduction in the ambient crust. Similarly, Falcone *et al.* (2018) numerically estimated for the 7 km deep borehole with radius of 0,16 m a heat extraction of 3 MW after 10 yr of water pumping. However, it should be emphasized that our estimates of maximum heat extraction from the borehole can be made in such a simple way because we approximate the boundary condition by $T_a(z) \to T_0$ and, therefore, it is easy to evaluate the total heat flow from the crust to the borehole.

2.2 Energy balance between circulating water in the borehole and the ambient ground

In more general cases, where cooling of the outer wall of the borehole by the downward flow of water is not sufficiently intensive, we do not have an estimate of the crust temperature close to the borehole and thus we must study the energy balance between the circulating water in the borehole and the ambient crust. Following, for example, Pan *et al.* (2019), Luo *et al.* (2020) and Zhao *et al.* (2020), we will deal with quasi-steady states. The simplest analytical one-layer models will be presented first and the results will then be generalized to analytical multilayer models that will approximate a general depth dependence of material parameters of either the crust or the borehole construction.

2.2.1 Ideal heat exchangers

To obtain the estimates of maximum possible heat extractions from a borehole, we start with the limiting case when the heat transfer between the downward and upward flows as well as the temperature differences between the ground at $r = a$ and the downward flow of water in the radial direction are negligible. In such a case, there is only energy balance between the heat advection of the downward flow of water and the heat conduction in the ground. This case is thus a model of an ideal borehole heat exchanger.

Model with constant material parameters (one-layer model)

The energy balance between the downward flow of water and the ambient ground can easily be expressed if we realize that the advection of heat in the water is given by the product of the specific heat capacity of the water c_w (in $\mathrm{J\,kgK^{-1}}$) with the amount of flowing water $\dot{m}$ (in $\mathrm{kg\,s^{-1}}$) and the temperature T_a. Therefore, the change of heat advection with depth in quasi-steady states is equal to $c_w \dot{m}\, \partial T_a/\partial z$, therefore,

$$c_w \dot{m} \frac{\partial T_a(z,t)}{\partial z} = k Q^* (T_b(z) - T_a(z,t)) \,, \tag{15}$$

where the right-hand side is the heat flow passing through the borehole wall per its unit length.

If the temperature T_b far from the borehole increases linearly with depth, that is, $T_b = T_0 + \beta z$, where T_0 is the surface temperature of the ground that wil be considered as a known constant and β is the geothermal gradient, we obtain the solution of eq. (15) in the form,

$$T_a(z,t) = T_0 + \beta z - \frac{\beta}{\lambda(t)} (1 - \exp(-\lambda(t) z)) + (T_a(0) - T_0) \exp(-\lambda(t) z) \,, \quad \lambda(t) \equiv \frac{k Q^*}{c_w \dot{m}} \,. \tag{16}$$

Here, we consider the temperature of inflow water $T_a(0)$ to be the known input parameter constant in time. If total depth of the borehole is d, the temperature $T_a(d, t)$ is then equal also to the temperature of the outflow of water, since the inner pipe is thermally isolated from the outer pipe. T_d is considered here as the (*a priori* unknown) output that changes in time.

The value of the parameter $\lambda(t)$ is controlled by the amount of water flow $\dot{m}$. Evidently,

$$\dot{m} \to 0 \Rightarrow \lambda \to \infty \Rightarrow T_a \to T_0 + \beta z \,,$$
$$\dot{m} \to \infty \Rightarrow \lambda \to 0 \text{ and } \exp(-\lambda z) \doteq 1 - \lambda z \Rightarrow T_a(z,t) \to T_a(0) \,.$$

The total heat extraction $Q_{\mathrm{tot}}(t)$ from the borehole reaching the depth d is

$$\begin{aligned} Q_{\mathrm{tot}}(t) &= c_w \dot{m} (T_a(d,t) - T_a(0)) \\ &= \frac{k Q^*}{\lambda(t)} \left[\beta \left(d + \frac{\exp(-\lambda(t) d) - 1}{\lambda(t)} \right) + (T_a(0) - T_0)(\exp(-\lambda(t) d) - 1) \right], \end{aligned} \tag{17}$$

and the limiting cases are

$$\dot{m} \to 0 \Rightarrow \lambda \to \infty \Rightarrow Q_{tot} \to 0 \,,$$
$$\dot{m} \to \infty \Rightarrow \lambda \to 0 \text{ and } \exp(-\lambda d) \doteq 1 - \lambda d + (\lambda d)^2/2 \Rightarrow Q_{\mathrm{tot}} \to k Q^* \left(\frac{\beta d^2}{2} + (T_0 - T_a(0)) d \right) \,,$$

which is in agreement with the estimates in the previous section (eq. 14) that are based on averaging the temperature in the borehole over depth.

It is simple to inverse eqs (16) and (17) to obtain $T_a(0, t)$ as the output for the inputs $T_a(d)$ or Q_{tot}, respectively, where the new inputs will now be constant to keep the quasi-steady approximation

$$T_a(0,t) = T_a(d) \exp(\lambda(t) d) + T_0 (1 - \exp(\lambda(t) d)) - \beta z \exp(\lambda(t) d) + \frac{\beta}{\lambda(t)} (\exp(\lambda(t) d) - 1) \,, \tag{18}$$

$$T_a(0,t) = \frac{1}{c_w \dot{m}} \frac{1}{\exp(-\lambda(t) d) - 1} Q_{\mathrm{tot}} + T_0 - \beta \left(\frac{d}{\exp(-\lambda(t) d) - 1} + \frac{1}{\lambda(t)} \right) \,. \tag{19}$$

Finally, we can also express $T_a(d, t)$ as the output for the constant input Q_{tot} as well as $Q_{\mathrm{tot}}(t)$ as the output for the constant input $T_a(d)$,

$$T_a(d,t) = \frac{1}{c_w \dot{m}} \frac{\exp(-\lambda(t) d)}{\exp(-\lambda(t) d) - 1} Q_{\mathrm{tot}} + T_0 - \beta \left(\frac{d}{\exp(-\lambda(t) d) - 1} + \frac{1}{\lambda(t)} \right) \,. \tag{20}$$

$$Q_{\mathrm{tot}}(t) = c_w \dot{m} \frac{\exp(-\lambda(t) d) - 1}{\exp(-\lambda(t) d)} \left[T_a(d) - T_0 + \beta \left(\frac{d}{\exp(-\lambda(t) d) - 1} + \frac{1}{\lambda(t)} \right) \right] \,. \tag{21}$$

The influence of $\dot{m}$ on the temperature and the extraction of heat is illustrated in Figs 2 and 3 for $Q^* = 1.2$, which roughly corresponds to the borehole with radius 0,15 m after two years of constant water pumping (see also Fig. 1), $k = 3\,\mathrm{W\,mK^{-1}}$, $c_w = 4{,}18\,\mathrm{kJ\,kgK^{-1}}$ and $\beta = 30\,\mathrm{K\,km^{-1}}$. One can clearly see that even a relatively small pumping of water with $\dot{m}$ of the order of $1\,\mathrm{kg\,s^{-1}}$ can produce about 1 MW of

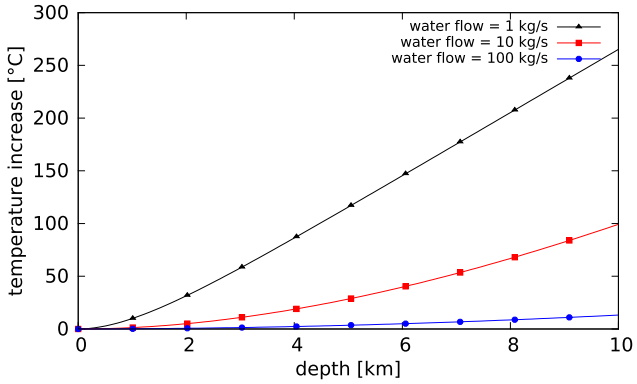

Figure 2. Theoretical maximum increase of temperature in the borehole up to a depth of 10 km. The amount of pumped water $\dot{m}$ is 1, 10 and 100 kg s^{-1}.

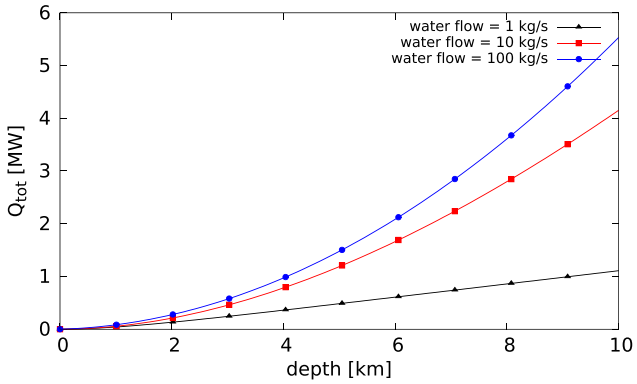

Figure 3. Theoretical maximum extraction of heat from the borehole as a function of its depth. The amount of pumped water $\dot{m}$ is 1, 10 and 100 kg s^{-1}.

energy in the case of a superdeep borehole of about 10 km depth. Emphasize again that these are maximal estimates since the exchange of heat between the downward and upward flows is neglected and a decrease of β with depth is not taken into account.

Multilayered model

In the case of a more complex crust model, where the thermal conductivity k , the thermal diffusivity κ and the geothermal gradient β are depth dependent, we can employ a layered model (with k , κ and β to be constant within each layer) to approximate such a situation. Emphasize that we again do no take vertical (axial) heat flow into account not only inside the layers but also on the interfaces between the layers. This is consistent, for example, with Karabetoglu *et al.* (2021), who demonstrated that interlayer heat transfer is almost completely negligible. If T_a^i and T_b^i denote the values of the temperatures T_a and T_b on the upper interface $z = z_i$ of the i th layer, the temperature T_a in the i th layer is given by the relation

$$T_a(z,t) = T_b^i + \beta_i(z - z_i) - \frac{\beta_i}{\lambda_i(t)}\left(1 - \exp(-\lambda_i(t)(z - z_i))\right) - (T_b^i - T_a^i(t))\exp(-\lambda_i(t)(z - z_i)) \,, \quad \lambda_i(t) \equiv \frac{k_i Q_i^*}{c_w \dot{m}} \,. \tag{22}$$

Now we will consider the temperature of inflowing water T_a^1 to be the known constant input quantity, moreover, $T_b^1 = T_0$ for $z = z_1 = 0$, and thus it is easy to express the temperature of downward flow of water for any depth using eq. (22). For $i > 1$, it holds:

$$T_b^i = T_b^1 + \sum_{j=1}^{i-1} \beta_j(z_{j+1} - z_j) \,, \tag{23}$$

$$\begin{aligned} T_a^i(t) = M_{i-1}(t)\Big[\ldots\Big[M_2(t)\Big[M_1(t)T_a^1 + (1 - M_1(t))(T_b^1 - \frac{\beta_1}{\lambda_1(t)}) + \beta_1(z_2 - z_1)\Big] \\ +(1 - M_2(t))(T_b^2 - \frac{\beta_2}{\lambda_2(t)}) + \beta_2(z_3 - z_2)\Big]\ldots\Big] \\ +(1 - M_{i-1}(t))(T_b^{i-1} - \frac{\beta_{i-1}}{\lambda_{i-1}(t)}) + \beta_{i-1}(z_i - z_{i-1}) \,, \quad M_i(t) \equiv \exp(-\lambda_i(t)(z_{i+1} - z_i)) \,. \end{aligned} \tag{24}$$

If we denote

$$S_i(t) = (1 - M_i(t))(T_b^i - \frac{\beta_i}{\lambda_i(t)}) + \beta_i(z_{i+1} - z_i) \,, \tag{25}$$

we can rewrite the formula (24) in a more compact form

$$T_a^i(t) = \prod_{j=1}^{i-1} M_{i-j}(t) T_a^1 + \sum_{k=1}^{i-2} \left(\prod_{j=1}^{i-1-k} M_{i-j}(t) S_k(t) \right) + S_{i-1}(t) \,. \tag{26}$$

Note that if we need to evaluate the temperature T_a inside a layer, it is possible to formally add the interface to the depth of interest and use again eq. (26).

In a model consisting of N layers the temperature of outflowing water T_a^{N+1} is, therefore,

$$T_a^{N+1}(t) = \prod_{j=1}^{N} M_{N+1-j}(t) T_a^1 + S(t), \quad \text{where} \quad S(t) = \sum_{k=1}^{N-1} \left(\prod_{j=1}^{N-k} M_{N+1-j}(t) S_k(t) \right) + S_N(t) \,. \tag{27}$$

The heat extraction Q_{tot} from the borehole is

$$Q_{\text{tot}}(t) = c_w \dot{m} (T_a^{N+1}(t) - T_a^1) = c_w \dot{m} \left[\left(\prod_{j=1}^{N} M_{N+1-j}(t) - 1 \right) T_a^1 + S(t) \right] . \tag{28}$$

Inversions of eqs (27) and (28) are

$$T_a^1(t) = \frac{(T_a^{N+1} - S(t))}{\prod_{j=1}^{N} M_{N+1-j}(t)} \,, \tag{29}$$

$$T_a^1(t) = \frac{Q_{\text{tot}} - c_w \dot{m} S(t)}{c_w \dot{m} \left(\prod_{j=1}^{N} M_{N+1-j}(t) - 1 \right)} \,. \tag{30}$$

Finally, the analogy of eqs (20) and (21) is

$$T_a^{N+1}(t) = \prod_{j=1}^{N} M_{N+1-j}(t) \frac{Q_{\text{tot}} - c_w \dot{m} S(t)}{c_w \dot{m} \left(\prod_{j=1}^{N} M_{N+1-j}(t) - 1 \right)} + S(t) \,, \tag{31}$$

$$Q_{\text{tot}}(t) = c_w \dot{m} \left[\frac{\prod_{j=1}^{N} M_{N+1-j}(t) - 1}{\prod_{j=1}^{N} M_{N+1-j}(t)} (T_a^{N+1} - S(t)) + S(t) \right] . \tag{32}$$

2.2.2 *Realistic heat exchangers*

Here, we will deal with realistic heat exchangers, where neither the heat flow between the inner and outer pipes nor the thermal resistance of the external borehole wall and the grout can be neglected.

Model with constant material parameters (one-layer model)

In what follows, we will distinguish between the temperature T_a on the side of the borehole wall and the temperature T_d of the water flowing downward; T_u will denote the temperature of the water flowing upward. The symbol R_e will be used to indicate the total thermal resistance of the external borehole wall together with the grout and R_i will denote the thermal resistance of the internal wall that separates the downward and upward flows of water, see Fig. 4. The energy balance is expressed by the following three equations:

$$c_w \dot{m} \frac{\partial T_d}{\partial z} = \frac{T_a(z) - T_d(z)}{R_e} + \frac{T_u(z) - T_d(z)}{R_i} \,, \tag{33}$$

that is, the water flowing downward is heated by the heat flow passing through both the external wall (and the grout) and the internal wall. The heat flow that passes through the external wall is equal to the heat flow from the crust, that is,

$$\frac{T_a(z) - T_d(z)}{R_e} = k Q^* (T_b(z) - T_a(z)) \,. \tag{34}$$

Finally, the water flowing upward is cooled by the heat flow passing through the internal wall, which can be expressed as

$$c_w \dot{m} \frac{\partial T_u}{\partial (-z)} = -\frac{T_u(z) - T_d(z)}{R_i} \,, \quad \text{or} \quad c_w \dot{m} \frac{\partial T_u}{\partial z} = \frac{T_u(z) - T_d(z)}{R_i} . \tag{35}$$

The three unknown quantities in eqs (33)–(35) are $T_a(z)$, $T_d(z)$ and $T_u(z)$. The question arises how to describe them in an analytical way.

It is straightforward to express $T_a(z)$ from eq. (34),

$$T_a(z) = \frac{R_e k Q^* T_b + T_d}{1 + R_e k Q^*} \,. \tag{36}$$

Subsequently, after putting $T_a(z)$ to eq. (33), we get a system of two equations of the first order for the temperatures of water T_d and T_u:

$$\frac{\partial T_d}{\partial z} = \mu(t) T_d + \nu T_u + \eta(t) T_b \,, \tag{37}$$

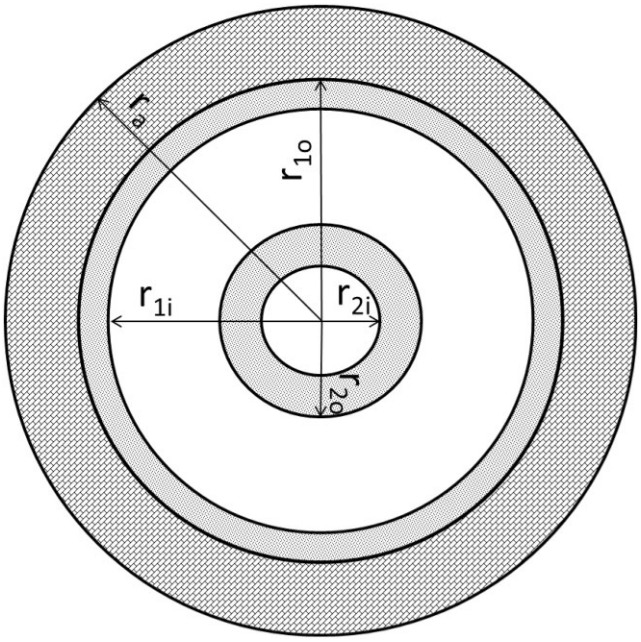

Figure 4. Borehole cross-section.

$$\frac{\partial T_u}{\partial z} = -\nu T_d + \nu T_u \,, \tag{38}$$

where

$$\mu(t) = \frac{1}{c_w \dot{m}} \left(\frac{1}{R_e(1 + R_e k Q^*)} - \frac{1}{R_e} - \frac{1}{R_i} \right) = \frac{1}{c_w \dot{m}} \left(\frac{-k Q^*}{1 + R_e k Q^*} - \frac{1}{R_i} \right) \,, \tag{39}$$

$$\nu = \frac{1}{c_w \dot{m} R_i} \,, \tag{40}$$

$$\eta(t) = \frac{k Q^*}{c_w \dot{m}(1 + R_e k Q^*)} \,. \tag{41}$$

Note that $\mu(t) + \nu + \eta(t) = 0$. Moreover, $\mu(t) \to -\lambda$, $\nu \to 0$ and $\eta(t) \to \lambda$ if $R_e \to 0$ and $R_i \to \infty$, which corresponds to the model studied in the previous Section 2.2.1.

Introduce the vector $\boldsymbol{T}(z, t)$ and the matrix $\boldsymbol{A}$ by

$$\boldsymbol{T}(z, t) \equiv \begin{pmatrix} T_d(z, t) \\ T_u(z, t) \end{pmatrix} \,, \quad \boldsymbol{A}(t) \equiv \begin{pmatrix} \mu(t) & \nu \\ -\nu & \nu \end{pmatrix} \,. \tag{42}$$

The solution of system eqs (37) and (38) can then be written in the form

$$\boldsymbol{T}(z, t) = (\exp(\boldsymbol{A}(t) z))\, \boldsymbol{C}(t) + \begin{pmatrix} T_0 + \beta z \\ T_0 + \beta z + \beta/\nu \end{pmatrix} \,, \tag{43}$$

where

$$\boldsymbol{C}(t) = \begin{pmatrix} C_1 \\ C_2(t) \end{pmatrix} = \begin{pmatrix} T_d(0) - T_0 \\ T_u(0, t) - T_0 - \beta/\nu \end{pmatrix}$$

is the vector of integration constants, where we used that $\exp(\boldsymbol{A}z)$ is the identity matrix for $z = 0$.

At $z = d$, where d is the thickness of the layer, we clearly have the boundary condition $T_d(d, t) = T_u(d, t)$, that is,

$$\begin{aligned} &(\exp(\boldsymbol{A}(t)\, d))_{11}\, C_1 + (\exp(\boldsymbol{A}(t)\, d))_{12}\, C_2(t) + T_0 + \beta d \\ &\quad = (\exp(\boldsymbol{A}(t)\, d))_{21}\, C_1 + (\exp(\boldsymbol{A}(t)\, d))_{22}\, C_2(t) + T_0 + \beta d + \beta/\nu \,, \end{aligned} \tag{44}$$

and thus

$$T_u(0, t) = M(t) T_d(0) + S(t) \,, \tag{45}$$

where

$$M(t) = \frac{(\exp(\boldsymbol{A}(t)\, d))_{21} - (\exp(\boldsymbol{A}(t)\, d))_{11}}{(\exp(\boldsymbol{A}(t)\, d))_{12} - (\exp(\boldsymbol{A}(t)\, d))_{22}} \,,$$

$$S(t) = (1 - M(t))T_0 + \left(1 + \frac{1}{(\exp(\boldsymbol{A}(t)\,d))_{12} - (\exp(\boldsymbol{A}(t)\,d))_{22}}\right)\beta/\nu\,,$$

and we will continue similarly as in the previous sections, that is,

$$Q_{\rm tot}(t) = c_w\dot{m}((M(t) - 1)T_d(0) + S(t))\,, \tag{46}$$

$$T_d(0, t) = \frac{T_u(0) - S(t)}{M(t)}\,, \tag{47}$$

$$T_d(0, t) = \frac{Q_{\rm tot} - c_w\dot{m}\,S(t)}{c_w\dot{m}(M(t) - 1)}\,, \tag{48}$$

and finally

$$T_u(0, t) = \frac{M(t)(Q_{\rm tot} - c_w\dot{m}\,S(t))}{c_w\dot{m}(M(t) - 1)} + S(t)\,, \tag{49}$$

$$Q_{\rm tot}(t) = c_w\dot{m}\left(\frac{M(t) - 1}{M(t)}(T_u(0) - S(t)) + S(t)\right)\,. \tag{50}$$

Special case:

If $R_i \to \infty$ then $\nu = 0$ and $\mu(t) = -\eta(t)$. Therefore, the formulae written above cannot be used due to the fraction β/ν. The results of Section 2.2 for the downflow temperature T_d can be used if λ is replaced by $\eta(t)$. The upflow temperature T_u is then constant and equal to $T_d(d)$.

Multilayered model

We consider a model consisting of N layers. Each layer is characterized by the values of the geothermal gradient of an unperturbed crust β_i and the values of the property matrix $\boldsymbol{A}^i$. Denote the $\boldsymbol{T}^i(t)$ and T_b^i values of $\boldsymbol{T}(t)$ and T_b on the upper interface of the i th layer $z = z_i$. The solution (43) in the i th layer can be rewritten to the form

$$\boldsymbol{T}(z, t) = (\exp(\boldsymbol{A}^i(t)(z - z_i)))\,\boldsymbol{C}^i(t) + \begin{pmatrix} T_b^i + \beta_i(z - z_i) \\ T_b^i + \beta_i(z - z_i) + \beta_i/\nu_i \end{pmatrix}\,. \tag{51}$$

Therefore,

$$\boldsymbol{C}^i(t) = \boldsymbol{T}^i(t) - \begin{pmatrix} T_b^i \\ T_b^i + \beta_i/\nu_i \end{pmatrix}\,. \tag{52}$$

The vector $\boldsymbol{T}$ and the unperturbed temperature T_b can thus be expressed on the next interface z_{i+1} simply by means of the scheme

$$\boldsymbol{T}^{i+1}(t) = \boldsymbol{M}^i(t)\boldsymbol{T}^i(t) + \boldsymbol{S}^i(t)\,, \quad T_b^{i+1} = T_b^i + \beta_i(z_{i+1} - z_i)\,, \quad T_b^1 \equiv T_0\,, \tag{53}$$

where

$$\boldsymbol{M}^i(t) = \exp(\boldsymbol{A}^i(t)(z_{i+1} - z_i)) \tag{54}$$

and

$$\boldsymbol{S}^i(t) = \begin{pmatrix} T_b^i + \beta_i(z_{i+1} - z_i) \\ T_b^i + \beta_i(z_{i+1} - z_i) + \beta_i/\nu_i \end{pmatrix} - \boldsymbol{M}^i(t)\begin{pmatrix} T_b^i \\ T_b^i + \beta_i/\nu_i \end{pmatrix}\,. \tag{55}$$

The relationship between $\boldsymbol{T}$ evaluated at the bottom of the borehole and at the surface is then given by a final scheme

$$\begin{aligned}\boldsymbol{T}^{N+1}(t) &= \boldsymbol{M}^N(t)(\boldsymbol{M}^{N-1}(t)(\ldots\boldsymbol{M}^2(t)(\boldsymbol{M}^1(t)\boldsymbol{T}^1(t) + \boldsymbol{S}^1(t)) + \boldsymbol{S}^2(t)) + \ldots) + \boldsymbol{S}^{N-1}(t)) + \boldsymbol{S}^N(t) \\ &= \prod_{i=1}^{N}\boldsymbol{M}^{N+1-i}(t)\boldsymbol{T}^1(t) + \sum_{j=1}^{N-1}\left(\prod_{i=1}^{N-j}\boldsymbol{M}^{N+1-i}(t)\boldsymbol{S}^j(t)\right) + \boldsymbol{S}^N(t) \equiv \boldsymbol{M}_{\rm tot}(t)\boldsymbol{T}^1(t) + \boldsymbol{S}_{\rm tot}(t)\,.\end{aligned} \tag{56}$$

Boundary conditions:

The boundary condition at $z = z_1$ is simply

$$(\boldsymbol{T}^1)_1 = T_d(z_1), \tag{57}$$

and the boundary condition at $z = z_{N+1}$,

$$T_d(z_{N+1}, t) = T_u(z_{N+1}, t) \tag{58}$$

can be written as

$$(\boldsymbol{M}_{\rm tot}(t))_{11}\,T_d(z_1) + (\boldsymbol{M}_{\rm tot}(t))_{12}\,T_u(z_1, t) + (\boldsymbol{S}_{\rm tot}(t))_1 = (\boldsymbol{M}_{\rm tot}(t))_{21}\,T_d(z_1) + (\boldsymbol{M}_{\rm tot}(t))_{22}\,T_u(z_1, t) + (\boldsymbol{S}_{\rm tot}(t))_2\,.$$

This means that

$$(\boldsymbol{T}^1)_2 \equiv T_u(z_1,t) = \frac{(\boldsymbol{M}_{\rm tot}(t))_{21} - (\boldsymbol{M}_{\rm tot}(t))_{11}}{(\boldsymbol{M}_{\rm tot}(t))_{12} - (\boldsymbol{M}_{\rm tot}(t))_{22}} T_d(z_1) + \frac{(\boldsymbol{S}_{\rm tot}(t))_2 - (\boldsymbol{S}_{\rm tot}(t))_1}{(\boldsymbol{M}_{\rm tot}(t))_{12} - (\boldsymbol{M}_{\rm tot})_{22}(t)}. \tag{59}$$

After denoting

$$M(t) = \frac{(\boldsymbol{M}_{\rm tot})_{21}(t) - (\boldsymbol{M}_{\rm tot}(t))_{11}}{(\boldsymbol{M}_{\rm tot}(t))_{12} - (\boldsymbol{M}_{\rm tot}(t))_{22}}\,, \quad S(t) = \frac{(\boldsymbol{S}_{\rm tot}(t))_2 - (\boldsymbol{S}_{\rm tot}(t))_1}{(\boldsymbol{M}_{\rm tot}(t))_{12} - (\boldsymbol{M}_{\rm tot})_{22}(t)} \tag{60}$$

temperature of the upward flow of water at the surface $T_u(z_1)$ and the total heat exctraction $Q_{\rm tot}$ from the borehole can be again expressed as

$$\boxed{T_u(z_1,t) = M(t)T_d(z_1) + S(t)\,, \quad Q_{\rm tot}(t) = c_w\dot{m}((M(t)-1)T_d(z_1) + S(t))}\,. \tag{61}$$

If the total heat extraction $Q_{\rm tot}$ (or the temperature of the outflow of water from the borehole $T_u(z_1)$) were considered as the constant input quantity, we could again use relevant formulae (47)–(50), because the formulae (61) are formally the same as eqs (45) and (46).

(De)coupling of the problems for downward and upward flows

Expressing T_u from eq. (37), (T_d z from eq. 38), we get after putting T_u in eq. (38), (T_d in eq. 37) two independent equations of the second order,

$$\frac{1}{\nu}\frac{\partial^2 T_d}{\partial z^2} - (1 + \frac{\mu(t)}{\nu})\frac{\partial T_d}{\partial z} + (\mu(t)+\nu)T_d = \frac{\eta(t)}{\nu}\frac{\partial T_b}{\partial z} - \eta(t)T_b\,, \tag{62}$$

$$\frac{1}{\nu}\frac{\partial^2 T_u}{\partial z^2} - (1 + \frac{\mu(t)}{\nu})\frac{\partial T_u}{\partial z} + (\mu(t)+\nu)T_u = \qquad -\eta(t)T_b\,. \tag{63}$$

If we multiply both equations by ν and use the relation $\nu + \mu(t) = -\eta(t)$, the systems (62) and (63) attain the form

$$\frac{\partial^2 T_d}{\partial z^2} + \eta(t)\frac{\partial T_d}{\partial z} - \nu\eta(t)T_d = \eta(t)\frac{\partial T_b}{\partial z} - \nu\eta(t)T_b\,, \tag{64}$$

$$\frac{\partial^2 T_u}{\partial z^2} + \eta(t)\frac{\partial T_u}{\partial z} - \nu\eta(t)T_u = \qquad -\nu\eta(t)T_b\,. \tag{65}$$

These equations must be supplemented by suitable boundary conditions on the surface $z = 0$ and at the bottom of the borehole $z = d$. We again assume that the temperature of the pumped water at the surface is equal to the surface temperature of the crust, therefore,

$$T_d(0) = T_a(0) = T_b(0) \equiv T_0\,. \tag{66}$$

Consequently, using eqs (33) and (35) we arrive at the following,

$$\frac{\partial T_d}{\partial z}(0) = \frac{\partial T_u}{\partial z}(0) = \frac{T_u(0) - T_0}{c_w\dot{m}R_i} \equiv (T_u(0) - T_0)\nu\,. \tag{67}$$

At the bottom of the borehole, the temperature of the water flowing downward is equal to the temperature of the water flowing upward,

$$T_d(d) = T_u(d)\,, \tag{68}$$

and thus the derivatives of these temperatures (see eqs 33, 36 and 41) are

$$\begin{aligned}\frac{\partial T_d}{\partial z}(d) &= \frac{1}{c_w\dot{m}R_e}(T_a(d) - T_d(d)) \\ &= \frac{1}{c_w\dot{m}R_e}\left(\frac{R_e k Q^* T_b(d) + T_d(d)}{1 + R_e k Q^*} - T_d(d)\right) = \eta(t)(T_b(d) - T_d(d))\,,\end{aligned} \tag{69}$$

$$\frac{\partial T_u}{\partial z}(d) = 0\,. \tag{70}$$

Eq. (64) can be supplemented by the boundary conditions (66) ($T_d(0) = T_0$) and (69), while the boundary conditions (67) ($\mathrm{d}T_u/\mathrm{d}z(0) = (T_u(0) - T_0)\nu$) and (70) can be added to eq. (65). Formally, the problems for T_d and T_u are thus decoupled and can be solved independently. However, there is a physical coupling hidden in the fact that the surface temperature of the downward flow T_d is used also in the surface value of the upward flow gradient $\mathrm{d}T_u/\mathrm{d}z$.

The homogeneous parts of eqs (64) and (65) are identical; their solution is

$$T^h_{d,u}(z) = A_{d,u}\exp(\omega_1 z) + B_{d,u}\exp(\omega_2 z)\,, \tag{71}$$

where $A_{d,u}$ and $B_{d,u}$ are integration constants and $\omega_{1,2}$ are the roots of the characteristic equation,

$$\omega_{1,2} = \frac{-\eta(t) \pm \sqrt{\eta(t)^2 + 4\nu\eta(t)}}{2} = \frac{\nu + \mu(t) \pm \sqrt{(\nu+\mu(t))^2 - 4\nu(\mu(t)+\nu)}}{2}\,. \tag{72}$$

Taking into account $T_b(z)$ in the form $T_b(z) = T_0 + \beta z$, the particular solution of eq. (64) is

$$T^p_d(z) = T_0 + \beta z \equiv T_b(z), \tag{73}$$

whereas the particular solution of eq. (65) is

$$T_u^p(z) = T_0 + \frac{\beta}{\nu} + \beta z \equiv T_b(z) + \frac{\beta}{\nu} . \tag{74}$$

We thus have arrived at

$$T_d(z) = A_d \exp(\omega_1 z) + B_d \exp(\omega_2 z) + T_0 + \beta z , \tag{75}$$

$$T_u(z) = A_u \exp(\omega_1 z) + B_u \exp(\omega_2 z) + T_0 + \frac{\beta}{\nu} + \beta z , \tag{76}$$

and after employing the boundary conditions mentioned above we get the following,

$$A_d = \frac{-\beta}{(\omega_1 + \eta(t))\exp(\omega_1 d) - (\omega_2 + \eta(t))\exp(\omega_2 d)} = -B_d ,$$
$$A_u = \frac{-\beta(\omega_2 - \nu)}{\omega_1(\omega_2 - \nu)\exp(\omega_1 d) - \omega_2(\omega_1 - \nu)\exp(\omega_2 d)} = -\frac{\omega_2 - \nu}{\omega_1 - \nu} B_u .$$

In the case of the N-layered model, we will write in each layer

$$T_d^i(z) = A_d^i \exp(\omega_1 z) + B_d^i \exp(\omega_2 z) + T_b^i + \beta_i z , \tag{77}$$

$$T_u^i(z) = A_u^i \exp(\omega_1 z) + B_u^i \exp(\omega_2 z) + T_b^i + \frac{\beta_i}{\nu_i} + \beta_i z . \tag{78}$$

There are $4N$ unknown integration constants $A_{d,u}^i$, $B_{d,u}^i$, but we can employ four boundary conditions on the surface and bottom of the borehole, and, moreover, the temperature must be continuous on each internal interface, that is,

$$T_d^i(z_{i+1}) - T_d^{i+1}(z_{i+1}) = 0 , \quad T_u^i(z_{i+1}) - T_u^{i+1}(z_{i+1}) = 0 , \quad i = 1, 2, \ldots, N-1 . \tag{79}$$

To complete a system of required equations for the integration constants, we need to write other $2N-2$ conditions on internal boundaries.

First, we write conditions for the derivatives $\tau_d(z) \equiv \mathrm{d}T_d(z)/\mathrm{d}z$ and $\tau_u \equiv \mathrm{d}T_u(z)/\mathrm{d}z$. It is clear from eqs (37) and (38) that these derivatives are not continuous on internal boundaries due to jumps of the material coefficients $\mu(t)$, ν and $\eta(t)$ on the internal layer interfaces. Since the continuity of temperature eq. (79) holds, we may write for $i = 1, 2, \ldots, N-1$

$$\tau_d^{i+1}(z_{i+1}) - \tau_d^i(z_{i+1}) = (\mu_{i+1}(t) - \mu_i(t))T_d^i(z_{i+1}) + (\nu_{i+1} - \nu_i)T_u^i(z_{i+1}) + (\eta_{i+1}(t) - \eta_i(t))T_b^i(z_{i+1}) \tag{80}$$

and

$$\tau_u^{i+1}(z_{i+1}) - \tau_u^i(z_{i+1}) = -(\nu_{i+1} - \nu_i)T_d^i(z_{i+1}) + (\nu_{i+1} - \nu_i)T_u^i(z_{i+1}) . \tag{81}$$

The consequence of the material coefficient jumps is, therefore, that calculations of downward and upward flow temperatures employing the conditions (80) and (81) are coupled.

In order to decouple the interface conditions, we go back to the relations (64), (65), (71), (75) and (76). Since T_d, T_u and T_β are continuous on internal layer interfaces, it is also clear that

$$T_d^h \equiv \frac{1}{\nu\eta(t)} \frac{\partial^2 T_d^h}{\partial z^2} + \frac{1}{\nu} \frac{\partial T_d^h}{\partial z} \tag{82}$$

and

$$T_u^h + \beta\nu \equiv \frac{1}{\nu\eta(t)} \frac{\partial^2 T_u^h}{\partial z^2} + \frac{1}{\nu} \frac{\partial T_u^h}{\partial z} + \beta\nu \tag{83}$$

must be continuous. Therefore, the continuity of the right-hand sides of eqs (82) and (83) can replace the conditions (80) and (81).

3 VALIDATION OF THE METHOD AND PARAMETRIC STUDIES

First, the thermal resistance from the borehole wall to the fluid in the outer pipe R_e and the thermal resistance between the outer and the inner pipes fluid R_i must be determined. We use their magnitude calculated from the relations

$$R_e = \frac{1}{2\pi k_g} \ln\left(\frac{r_a}{r_{1o}}\right) + \frac{1}{2\pi k_{p1}} \ln\left(\frac{r_{1o}}{r_{1i}}\right) + \frac{1}{2\pi r_{1i} h_1} , \tag{84}$$

$$R_i = \frac{1}{2\pi k_{p2}} \ln\left(\frac{r_{2o}}{r_{2i}}\right) + \frac{1}{2\pi r_{2o} h_1} + \frac{1}{2\pi r_{2i} h_2} , \tag{85}$$

where r_a, r_{1o}, r_{1i}, r_{2o} and r_{2i} denote the outer radius of the grout, the outer and inner radii of the outer pipe and the outer and inner radii of the inner pipe, respectively, see Fig. 4. The symbols k_g, k_{p1} and k_{p2} are the thermal conductivities of the grout, the outer and inner pipes. Finally, h_1 and h_2 are the convective heat transfer coefficients for the outer and inner pipes. Following Pan *et al.* (2019), we calculate them employing the formula

$$h = \frac{k_f}{d}\left(\frac{(f/8)(Re - 1000)Pr}{1 + 12.7(f/8)^{1/2}(Pr^{2/3} - 1)}\right) , \quad f = (0.79\ln(Re) - 1.64)^{-2} , \tag{86}$$

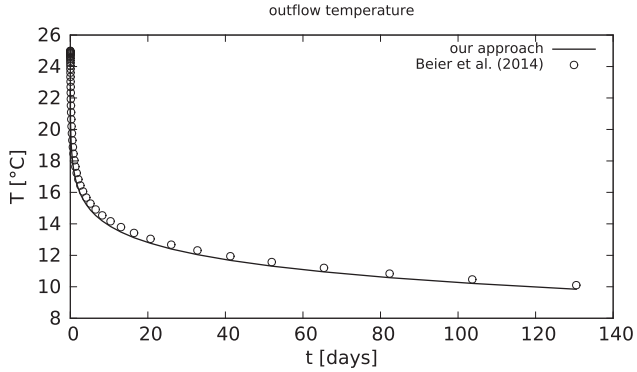

Figure 5. Temperatures of water outflowing from the 100 m deep borehole for $Q_{\rm tot}$ =5 kW and $\dot{m}$ =8.33 kg s^{-1}.

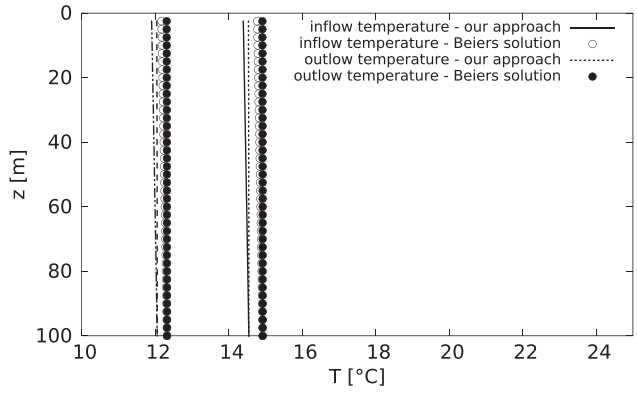

Figure 6. Temperature distribution of downflowing and upflowing water T_d and T_u, respectively, after 6.5 d (right-hand curves) and 33 d (left-hand curves) after the start of heating. Depth of the borehole is 100 m, $Q_{\rm tot}$ =5 kW and $\dot{m}$ =8.33 kg s^{-1}.

where k_f is the thermal conductivity of the circulating fluid, Re is the Reynolds number and Pr is the Prandtl number. Hydraulic diameter $d = 2(r_{1i} - r_{2o})$ in calculating h_1, and $d = 2r_{2i}$ in expressing h_2, respectively.

We tested our method against free software calculating temperatures in downflowing and upflowing water for *a priori* prescribed heat extraction. The software is based on analytical formulae in the Laplace domain (Beier *et al.* 2014). Fig. 5 shows the temperature of water outflowing from a 100 m deep borehole and entering into a heat pump for up to 130 d. Heat extraction of 5 kW and water flow of 8.33 kg s^{-1} were constant, other parameters of the borehole can be found in https://www.opengeosys.org/docs/benchmarks/heat-transport-bhe/3d_coaxial_deep_bhe/. Fig. 6 then demonstrates the temperature distribution of downflowing and upflowing water T_d and T_u, respectively, after 6.5 and 33 d after the start of heating. We also benchmarked our formulae with numerical calculations of Cai et al. (2022) for 2.2, 2.4, 2.6, 2.8 and 3 km deep boreholes, respectively, in the four-layers ground model. Constant temperature of inflow is 4 °C, surface temperature of the ground T_0 is 14.8 °C and the flow rate is 10 litres s^{-1}. Cai *et al.* (2022) reported the outflow temperatures after the end of heating season (120 d) for these boreholes to be 11.15, 12.51, 13.95, 15.47 and 17.06 °C, respectively. Our values are 10.65, 11.88, 13.18, 14.53 and 15.93 °C, respectively.

It is clear that in both tests we obtained slightly lower values of temperatures. This is the error of quasi-steady-state approximation. The formula (12) is precise if the temperature T_a is constant in time. However, in numerical experiments described in this paragraph, T_a slowly decreases, which causes an additional heat flow that is not taken into account in the quasi-steady-state approximation. Nevertheless, this error of several per cents is still sufficiently small (and probably below the errors caused, e.g. by uncertainties of the ground parameters) and thus we can conclude that our straightforward semi-analytical method provides reasonable fast estimates of water temperatures or heat extractions.

In the parametric studies presented in this section, we deal with a deep borehole reaching the depth of 3 km and a superdeep borehole of a depth of 10 km. Although there is no such superdeeep borehole employing geothermal energy yet, note that the depth of 10 km should be reached by recently started drilling in China. Presenting the results for such a borehole thus point to potential limits of heat extraction from a single superdeep borehole. To work with a realistic model of the crust, we divide its upper 10 km into five layers of the same thicknesses. Based on the background temperature profile T_b, we use thermal diffusivity and conductivity dependencies on temperature for an average crust (Whittington *et al.* 2009) to obtain their depth dependencies. Calculations of Q^* are made for the fixed borehole radius $r_a = 0.15$ m, the thermal diffusivities in Table 1 and $t = 500$ d. As shown in Table 1, Q^* increases with depth from about 1.17 to 1.26. All calculations

Table 1. Parameters of the crust model based on the thermal diffusivity profiles by Whittington *et al.* (2009).

Depth (km)	β (K km^{-1})	k (W mK^{-1})	κ (mm^2 s^{-1})	Q^*
0–2	29	3.8	2.00	1.17
2–4	27	3.6	1.75	1.19
4–6	25	3.4	1.50	1.22
6–8	23	3.2	1.25	1.24
8–10	21	3.0	1.00	1.26

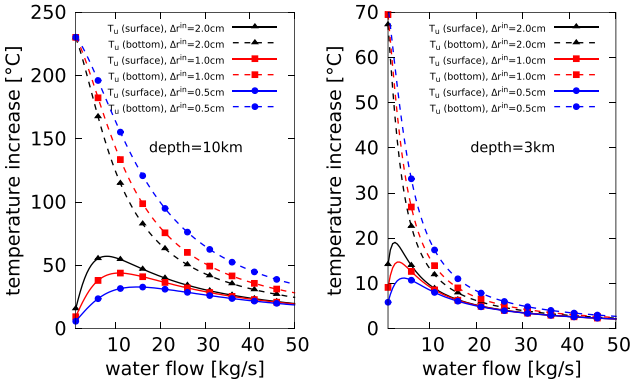

Figure 7. Temperatures $T_u - T_0$ at the borehole bottom and at the surface for the three thicknesses of the inner pipe wall. The boreholes are 10 km deep (left-hand panel) or 3 km deep (right-hand panel). Inner radius of the inner pipe r_{2i} is 5.5 cm.

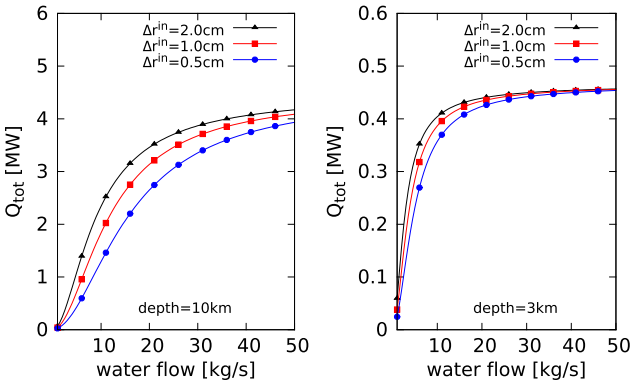

Figure 8. Total heat extraction from the 10 km deep borehole (left-hand panel) and the 3 km deep borehole (right-hand panel) for the three thicknesses of the inner pipe wall. Inner radius of the inner pipe r_{2i} is 5.5 cm.

presented in the following are based on formulae from the second subpart of Section 2.2.2. We use $r_a = 0.15$ m, $r_{1o} = 0.1$ m, $r_{1i} = 0.095$ m, $k_g = 1.5$ W mk^{-1}, $k_{p1} = 41$ W mk^{-1} and $k_{p2} = 0.4$ W mk^{-1}. Since the evaluation of explicit analytical formulae (56)–(61) is extremely fast, we can easily perform various parametric studies. Fig. 7 shows changes of temperature at the bottom of the borehole and the surface temperature of the outflowing water $T_u(0)$ with the change of the water flow $\dot{m}$ in cases, where $r_{2i} = 0.055$ m is fixed, but $r_{2o} = 0.075$, 0.065 and 0.06 m, respectively. We can see that the corresponding changes of the thermal resistance R_i (eq. 85) result in substantial changes of the temperatures shown. One can clearly see that $T_u(0)$ can reach only several tens of °C, and it is interesting that maximal outflow temperatures are reached for water flows of the order of 10 kg s^{-1} for the superdeep borehole but only several kg s^{-1} for the 3 km deep borehole. However, total heat extraction $Q_{\rm tot}$ increases with increasing $\dot{m}$ as shown in Fig. 8 and there is a saturation approximately at a level of 4 and 0.45 MW for the two studied borehole depths.

The thermal resistance R_i depends not only on the thickness of the inner pipe but also on its radius. Figs 9 and 10 show changes of temperature and total heat extraction with changes of r_{2i} for a water flow of 10 kg s^{-1}. One can see that the temperature T_u at the bottom increases with increasing r_{2i} but at the surface T_u decreases with increasing r_{2i} and thus $Q_{\rm tot}$ also decreases. This result can be explained by the fact that speed of water in the inner pipe decreases with increasing pipe radius and, therefore, the water flowing upward is more cooled during its journey from the bottom to the top of the borehole. The depth dependence of the temperature for $r_{2i} = 5.5$ cm is shown in Fig. 11.

We also tested the sensitivity of heat flow extraction on changes of R_e, but it is very small. For example, if we replace the thermal conductivity of the grout k_g by the thermal conductivity of the steel k_{p1}, the temperature at the bottom of the borehole increases only by

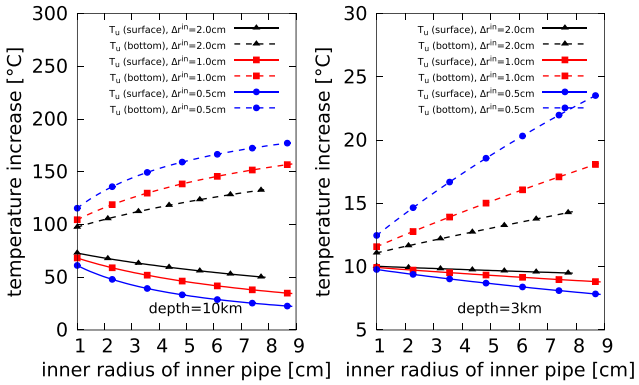

Figure 9. Temperatures $T_u - T_0$ at the borehole bottom and at the surface for the three thicknesses of the inner pipe wall and changing inner radius r_{2i} of the inner pipe. The boreholes are 10 km deep (left-hand panel) or 3 km deep (right-hand panel). Water flow $\dot{m}$ is 10 kg s^{-1}.

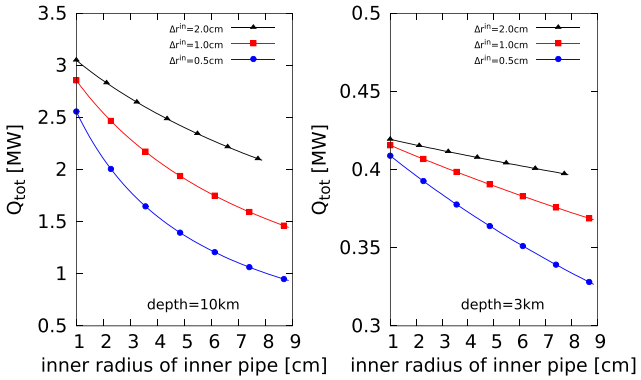

Figure 10. Total heat extraction from the 10 km deep borehole (left-hand panel) and the 3 km deep borehole (right-hand panel) for the three thicknesses of the inner pipe wall and changing inner radius r_{2i} of the inner pipe. Water flow $\dot{m}$ is 10 kg s^{-1}.

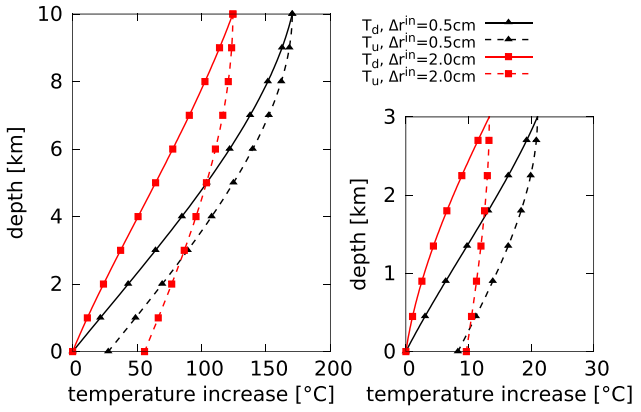

Figure 11. Depth dependencies of temperatures $T_d - T_0$ and $T_u - T_0$ for the two thicknesses of the inner pipe wall. The boreholes are 10 km deep (left-hand panel) or 3 km deep (right-hand panel). Inner radius of the inner pipe r_{2i} is 5.5 cm and water flow $\dot{m}$ is 10 kg s^{-1}.

several degrees and a change of $Q_{\rm tot}$ is negligible. The physical reason is based on the fact that the heat flow from the crust to the borehole is proportional to $T_b - T_a$; changes of R_e influence T_a, but changes of the difference $T_b - T_a$ remain relatively small.

4 CONCLUSIONS

We present a new method that enables us to calculate quasi-static heat extraction from coaxial boreholes in realistic layered crust models. Potentially changing thermal resistivities of the borehole wall and the inner pipe were also included. Our approach consists of the two independent steps. First, we deal with the heat conduction equation in axial symmetry outside a borehole and introduce the dimensionless quantity Q^* which is a function of the crustal thermal diffusivity, borehole radius and time. Then, the heat flow from the Earth's crust to the borehole is simply expressed by the multiplication of Q^* with the thermal conductivity of the crust and the difference between the

background temperature and that at the borehole wall. This quantity then enters the second step, where we analytically solve an energy-balance equation between the heat flow from the crust and changes of the temperature of the downflowing and upflowing fluids in the borehole. The matrix method is used to propagate the solution between the top and bottom of each layer and, subsequently, between the surface and borehole bottom. This enables us to incorporate boundary conditions and express the solution in any depth by means of a matrix multiplication.

We then performed parametric studies focused on the temperature of the water flow and, especially, the total heat extraction calculations from coaxial boreholes of the depths 3 and 10 km. The free parameters under study were the amount of water flow and thermal resistance of the inner pipe that separates the downflowing and upflowing pumped water. For an ideally insulating inner pipe, which is characterized by an infinite thermal resistance, the temperature of flow decreases but the total heat extraction increases with increasing amount of the water flow. However, in realistic models with finite thermal resistance controlled by the geometry of the pipe, the behaviour of flow temperature is more complicated. Total heat extraction is still increasing with increasing amount of flow but it is saturated for high flow amounts. The important parameter is the inner radius of the inner pipe. The smaller the radius is, the higher is the speed of upflowing water and, consequently, its temperature and total heat extraction. We also discuss changes of total heat extraction from the borehole due to changes of the insulation quality of the inner pipe when amount of pumped water is fixed.

ACKNOWLEDGMENTS

We thank two anonymous reviewers for their constructive and helpful reviews. The authors were supported by the project GAMA2 USMH AV ČR *Výměník tepla pro velmi hluboké geotermální vrty.*

DATA AVAILABILITY STATEMENT

No new data were generated or analysed in support of this research. The code can be available as part of the final publication.

REFERENCES

Beier, R.A., Acuña, J., Mogensen, P. & Palm, B., 2014. Transient heat transfer in a coaxial borehole heat exchanger, *Geothermics,* **51,** 470–482.

Brown, C.S., Doran, H., Kolo, I., Banks, D. & Falcone, G., 2023a. Investigating the influence of groundwater flow and charge cycle duration on deep borehole heat exchangers for heat extraction and borehole thermal energy storage, *Energies,* **16,** 2667, doi:10.3390/en16062677.

Brown, C.S., Kolo, I., & Banks, D., 2023b. Investigating scalability of deep borehole heat exchangers: numerial modelling of arrays with varied modes of operation, *Renew. Energy,* **202,** 442–452.

Cai, W., Wang, F., Jiang, J., Wang, Z., Liu, J. & Chen, C., 2022. Long-term performance evaluation and economic analysis for deep borehole heat exchanger heating system in Weihe Basin, *Front. Earth Sci.,* **10,** 806416, doi:10.3389/feart.2022.806416.

Carslaw, H.S. & Jaeger, J.C., 1959. *Conduction of Heat in Solids,* Oxford University Press.

Claesson, J. & Eskilson, P., 1988. Conductive heat extraction to a deep borehole: thermal analyses and dimensioning rules, *Energy,* **13,** 509–527.

Diersch, H.-J.G., Bauer, D., Heidemann, W., Rühaak, W. & Schätzl, P., 2011a. Finite element modeling of borehole heat exchanger systems, Part 1. Fundamentals, *Comput. Geosci.,* **37,** 1122–1135.

Diersch, H.-J.G., Bauer, D., Heidemann, W., Rühaak, W. & Schätzl, P., 2011b. Finite element modeling of borehole heat exchanger systems, Part 2. Numerical simulation, *Comput. Geosci.,* **37,** 1136–1147.

Eskilson, P., 1987. *Thermal Analysis of Heat Extraction Boreholes,* PhD thesis, University of Lund, Sweden.

Falcone, G., Liu, X., Okech, R.R., Seyidov, F. & Teodoriu, C., 2018. Assessment of deep geothermal energy exploitation methods: The need for novel single-well solutions, *Energy,* **160,** 54–63.

Fang, L., Diao, N., Shao, Z., Zhu, K. & Fang, Z., 2018. A computationally efficient numerical model for heat transfer simulation of deep borehole heat exchangers, *Energy Build.,* **167,** 79–88.

He, Y. & Bu, X., 2020. A novel enhanced deep borehole heat exchanger for building heating, *Appl. Therm. Eng.,* **178,** 115643, doi:10.1016/j.applthermaleng.2020.115643.

Iry, S. & Rafee, R., 2019. Transient numerical simulation of the coaxial borehole heat exchanger with the different diameters ratio, *Geothermics,* **77,** 158–165.

Jiao, K., Sun, C., Yang, R., Yu, B. & Bai, B., 2021. Long-term heat transfer analysis of deep coaxial borehole heat exchangers via an improved analytical model, *Appl. Therm. Eng.,* **197,** 117370, doi:10.1016/j.applthermaleng.2021.117370.

Karabetoglu, S., Ozturk, Z.F., Kaslilar, A., Juhlin, C. & Sisman, A., 2021. Effect of layered geological structures on borehole heat transfer, *Geothermics,* **91,** 102043, doi:10.1016/j.geothermics.2021.102043.

Kohl, T., Brenni, R. & Eugster, W., 2002. System performance of a deep borehole heat exchanger, *Geothermics,* **31,** 687–708.

Le Lous, L., Larroque, F., Dupuy, A. & Moignard, A., 2015. Thermal performance of a deep borehole heat exchanger: Insight from a synthetic coupled heat and flow model, *Geothermics,* **57,** 157–172.

Li, J. *et al.*, 2021. Heat extraction model and characteristics of coaxial deep borehole heat exchanger, *Renew. Energy,* **169,** 738–751.

Liu, J., Wang, F., Cai, W., Wang, Z. & Li, Ch., 2020. Numerical investigation on the effects of geological parameters and layered subsurface on the thermal performance of medium-deep borehole heat exchanger, *Renew. Energy,* **149,** 384–399.

Luo, Y., Cheng, N. & Xu, G., 2022. Analytical modeling and thermal analysis of deep coaxial borehole heat exchanger with stratified-seepage-segmented finite line source method (S^3-FLS), *Energy Build.,* **257,** 111795, doi:10.1016/j.enbuild.2021.111795.

Luo, Y., Guo, H., Meggers, F. & Zhang, L., 2019. Deep coaxial borehole heat exchanger: analytical modeling and thermal analysis, *Energy,* **185,** 1298–1313.

Luo, Y., Guozhi, X. & Yan, T., 2020. Performance evaluation and optimization design of deep ground source heat pump with non-uniform internal insulation based on analytical solutions, *Energy Build.,* **229,** 110495, doi:10.1016/j.enbuild.2020.110495.

Ma, L., Zhao, Y., Yin, H., Zhao, J., Li, W. & Wang, H., 2020. A coupled heat transfer model of medium-depth downhole coaxial heat exchanger based on the piecewise analytical solution, *Energy Convers. Manage.,* **204,** 112308, doi:10.1016/j.enconman.2019.112308.

Morchio, S. & Fossa, M., 2019. Thermal modeling of deep borehole heat exchangers for geothermal applications in densely populated urban areas, *Therm. Sci. Eng. Prog.,* **13,** 100363, doi:10.1016/j.tsep.2019.100363.

Pan, S., Kong, Y., Chen, Ch., Pang, Z. & Wang, J., 2020. Optimization of the utilization of deep borehole het exchangers, *Geotherm. Energy,* **8,** 20, doi:10.1186/s40517-020-0161-4.

Pan, A., Lu, L., Cui, P. & Jia, L., 2019. A new analytical heat transfer model for deep borehole heat exchangers with coaxial tubes, *Int. J. Heat Mass Transf.,* **141,** 1056–1065.

Song, X., Wang, G., Shi, Y., Li, R.,,, Zheng, R., Wang, Y. & Li, J., 2018. Numerical analysis of heat extraction performance of a deep coaxial borehole heat exchanger geothermal system, *Energy,* **164,** 1298–1310.

Whittington, A.G., Hofmeister, A.M. & Nabelek, P.I., 2009. Temperature-dependent thermal diffusivity of the Earth's crust and implications for magmatism, *Nature,* **458,** 319–321.

Zhao, Y., Pang, Z., Huang, Y. & Ma, Z., 2020. An efficient hybrid model for thermal analysis of deep borehole heat exchangers, *Geotherm. Energy,* **8,** 31, doi:10.1186/s40517-020-00170-z.